Available online at www.sciencedirect.com
SCIENCE DIRECT
Polymer 46 (2005) 6369–6379
polymer
www.elsevier.com/locate/polymer

Strain hardening modulus as a measure of environmental stress crack resistance of high density polyethylene

L. Kurelec[a,*], M. Teeuwen[b], H. Schoffeleers[b], R. Deblieck[b]

[a]*Material Development Department, SABIC—Europetrochemicals, Research and Development, Oude Postbaan 1, P.O. BOX 319; 6160AH Geleen, The Netherlands*
[b]*DSM Research, P.O. Box 18, 6160 MD Geleen, The Netherlands*

Received 22 December 2004; received in revised form 30 March 2005; accepted 19 May 2005
Available online 5 July 2005

Abstract

In this paper it is shown that the resistance to slow crack propagation in polyethylene can be predicted from a simple tensile measurement performed at 80 °C. It is shown that for different types of polyethylene homopolymers and copolymers the slope of a tensile curve above its natural draw ratio (i.e. strain hardening) correlates well with the measured stress crack resistance. The data presented in this paper confirm that the slow crack resistance in polyethylene is determined by the failure of the fibrils within the craze, which is shown to be determined by the strain hardening of a tensile curve. A material with a strong strain hardening will reduce the strain rate and consequently the time to failure will be strongly increased. Considering the fact that the slow crack resistance of polyethylene is usually assessed by tedious and time consuming testing methods performed on the notched samples in contact with specific fluids, the findings reported in this publication offer a possibility to assess the information on slow crack propagation in much simpler and faster way.

Keywords: HDPE; Slow crack propagation; Stress–strain

1. Introduction

Slow crack resistance, often estimated by environmental stress crack resistance (ESCR) tests, is an important performance parameter for different applications of HDPE, from the blow moulding segment like bottles and containers up to the highly demanding applications like water and gas pipes.

Slow crack resistance in polyethylene has been reported extensively in the literature [1–9,19]. Resistance of slow crack growth is considered when the applied stress on a specimen (product) is much lower than the yield stress and in the presence of bulk inhomogeneities (scratches, pigments, catalyst residues). The overall failure is brittle and it proceeds via a so-called deformation zone, which is formed at the tip of a crack. Such a deformation zone consists of microscopic cavities (voids) that will grow and join up to form a cross-tied network of essentially fibrillar entities usually referred to as craze [10–12]. The development of the damage zone up to the fracture of the fibrils within a craze is usually considered to proceed through three main stages, i.e. initiation, propagation and total fracture. The initiation step includes the formation of the deformation zone, which is strongly associated with the yield stress and stiffness of a material [4]. Once the damage zone is formed it will start to grow; i.e. to propagate. The propagation is usually associated with two main phenomena (a) stretching and subsequent weakening of fibrils and (b) a growth of the fibrillated area by propagation of the craze, i.e. transformation of material from the elastically deformed state to the plastically deformed, fibrillated state (lateral growth of a craze) [8,9,13]. The former process (stretching of fibrils) is believed to be governed by the disentanglement process of (tie) molecules [13–15] while the latter process (propagation of the deformation zone) involves yielding (plastic deformation occurring at the point of stress concentration) [4].

Slow crack growth in polyethylene is shown to be highly dependent on different molecular and morphological parameters like molecular mass [16–20] and molecular

* Corresponding author. Tel.: +31 464764326; fax: +31 464760503.
E-mail address: lada.kurelec@sabic-europe.com (L. Kurelec).

0032-3861/$ - see front matter © 2005 Elsevier Ltd. All rights reserved.
doi:10.1016/j.polymer.2005.05.061

Table 1
Material characteristics of HDPEs used in this study

Grades	Application	Density (kg/m^3)	MFR 5 (10 g/min)	MFR 21 (10 g/min)	M_n (kg/mol)	M_w (kg/mol)	M_z (kg/mol)	Comonomer	SCB/ 1000C[a]	ESCR (h)
Cr HDPE1	Blow molding	944	0.8	20	13	210	1056	Butene	4.1	58
Cr HDPE2	Blow molding	944	0.8	19	11	177	1023	Butene	3.8	103
Cr HDPE3	Blow molding	958	0.9	22	8	215	2200	Butene	0.7	10
Cr HDPE4	Blow molding	954	0.9	20	11	175	1300	Butene	1.7	20
Cr HDPE5	Blow molding	945	0.9	20	10	190	1600	Butene	4.1	50
Cr HDPE6	Blow molding	947	0.9	20	10	200	1800	Butene	4.1	47
Cr HDPE7	Blow molding	947	0.9	20	9	195	1750	Hexene	3.5	112
Cr HDPE8	Pipe PE80	949	0.9	17	8	245	1300	Butene	4.9	300
biHDPE1	Pipe PE80	956	0.5	10	10	230	1200	Butene	1.5	1000
biHDPE2	Pipe PE100	959	0.3	8	11	280	1500	Hexene	2.5	>2000
Cr HDPE9	Blow molding	952	–	9	9	300	2300	Butene	1.7	144;89;123

[a] Short chain branching (SCB) determined by ^{1}H NMR.

mass distribution [5,6], comonomer content [21], its type [22] and the chemical composition distribution [23] as well as the macroscopic density (crystallinity).

Because slow crack growth is a very slow process, testing of such long-term properties is accelerated by usage of a non-ionic surfactant environment as well as an elevated temperature leading to the values usually referred to as an environmental stress crack resistance (ESCR). Such tests are claimed to be designed in such a way that the failure mechanism is the same one as encountered during slow crack propagation [24]. The role of surfactants in the acceleration of slow crack propagation failure has been studied and it has been shown that surfactants facilitate craze growth by plasticizing the amorphous phase [25] and promote fracture by interacting with the crystalline region of the fibrils at the base of the craze where it acts as a lubricant for chain sliding [7,26]. Another parameter used for the acceleration of slow crack propagation measurements is elevated temperature, which provides enhanced chain mobility within a crystal (α-relaxation process [27]) facilitating solid-state chain diffusion through the crystalline phase and subsequently crystal shear [28]. In this context it should be mentioned that the theory of Kramer et al. [29] on craze propagation in glassy amorphous polymers attributes the ease of formation of internal surface to a polymeric surface tension that is determined by the sum of secondary interactions and the contribution of load bearing chains that need to be fractured or slip to form a surface. This elegant model explains the effect of a detergent and temperature as a decrease in the stress needed to propagate the craze, the so called craze stress. However, the possibility to shorten testing times by increasing temperature is limited because it is clear that brittle fracture has to be attained in order to make a reliable prediction of long term properties. If at the selected temperature the stress level is chosen too close to the yield stress of the material, ductile behaviour will predominate and obtained results will not be a measure of brittle failure [25].

Based on the above described principle of using surfactants and increased temperatures a number of different testing procedures have been developed and are widely used in industry. Examples are the bent strip test [30] or full notch creep test (FNCT) [24,31]. The problem often encountered with such testing methods is their poor long-term reproducibility, high sensitivity on surfactant quality and rather critical specimen preparation (namely notching procedure) [32].

In mid nineties O' Connell [33,34] et al. approached the slow crack propagation step via the creep rate deceleration of drawn polyethylene samples. In their approach they simulated the fibrillar structure within a craze by a tensile bar drawn to its natural draw ratio. They found a uniform relation between the creep rate deceleration of the drawn material and the growth as well as the failure of the craze. Cawood et al. showed that there is a direct relationship between the creep rate deceleration with a standard (accelerated) ESCR measurement [35,36]. These results clearly showed that the creep of the fibrils within a craze is a determining factor determining slow crack growth in polyethylene.

In this paper it will be shown that it is equivalent and experimentally more simple to use stress–strain curves at the identical deformation rates to assess long term performance (ESCR) of HDPE products. The parameter which we will link to ESCR performance is the measure of resistance against further deformation above the natural draw ratio i.e., the slope of the strain hardening part of a stress–strain curve, notably at elevated temperature ($\sim$80 °C). It will be demonstrated that this amount of strain hardening is highly sensitive to subtle molecular differences shown to be of influence on slow crack propagation in HDPE.

The method will be elaborated on two categories of HDPEs where ESCR plays an important role: Phillips based HDPE grades and bimodal Ziegler-Natta grades. By selection of materials having different molecular structure it will be shown that tensile tests at elevated temperature can discriminate very subtle molecular differences leading to variation in ESCR performance.

2. Experimental part

2.1. Materials

For this study a range of HDPEs, unimodal, molecularly broad Phillips catalyst based HDPEs (CrHDPE) as well as bimodal Ziegler-Natta HDPEs (biHDPEs), have been selected.

The material characteristics of the selected grades are given in Table 1.

MFR 5 and MFR 21 are melt flow rate indices measured at 190 °C under the weighted piston having a total mass of 5 and 21 kg, respectively, according to ISO 1133 standard.

Average molar masses (M_n, M_w, M_z) are determined by size exclusion chromatography (SEC) in 1,2,4-trichlorobenzene at 140 °C. Typical error estimates (± 2 sigma values) of this measurement are M_n(15–20%), M_w(10%), M_z(10–20%).

The amount of short chain branches (SCB) expressed per 1000 C atoms determined by ^{1}H NMR.

It can be seen in Table 1 that all CrHDPEs used in this study possess comparable MFRs and relatively small differences in molar mass values (at least if one considers the average error in the SEC apparatus). The most prominent differences between these samples are in density and comonomer type.

2.2. Molecular characterisation

Samples CrHDPE1 and CrHDPE 2 exhibit the same MFRs and density, while ESCR values as measured by the accelerated ESCR test differ significantly. This phenomenon is often encountered for Phillips catalysed products, which are characterised by a very broad molar mass distribution (M_w/M_n between 15 and 30) as well as a broad chemical composition distribution (CCD). In order to elaborate on the molecular differences between these two samples a detailed molecular characterisation of these particular samples has been performed.

Molecular characterisation of CrHDPE1 and CrHDPE 2 has been performed in two steps. Chemical composition distribution (CCD) curves, showing short chain branching distribution, have been obtained by analytical temperature rising elution fractionation (a-TREF) similar to the one used by Wild [38]. Based on a-TREF results preparative temperature rising elution fractionation (p-TREF) has been performed in order to collect TREF fractions, possessing different comonomer amount, which have been further analysed by SEC and ^{1}H NMR.

2.2.1. Analytical temperature rising elution fractionation (a-TREF)

a-TREF is performed in the solvent *ortho*-dichlorobenzene (ODCB) on a Chromosorb GAW-DMCS 80–100 MESH 0.15 m × 1/4″ × 4.0 mm SS column. The polymer concentration is 0.5% (mass/volume). The column is cooled from 140 till 20 °C with 1.5 °C/h. Next the column is put in the refrigerator at 2 °C for 1 night. Elution takes place continuously with 0.5 ml/min and a heating rate of 20 °C/h. The polymer concentration is detected by a Miran IR detector on a C–H stretch at a wavelength of 3.40 μm.

2.2.2. Preparative temperature rising fractionation (p-TREF)

Based on the analytical TREF curves temperatures for p-TREF have been selected. The selected temperature ranges in ODCB are: 63–85 °C, 85–93.3 °C, 93.3–96.5 °C and 96.5–113 °C.

2 g of the copolymer were mixed with 300 ml of xylene and were dissolved at 130 °C with the aid of a magnetic stirrer. The dissolved solution was then cooled down at a rate of 2 °C/h from 106 to 50 °C and then placed into a separating vessel. At the first fractionation temperature the total sample is vibrated for 0.5 h, filtrated off through a glass wool filter and the separating vessel is refilled with 300 ml preheated xylene. Rinsing takes place once by vibrating 0.5 h, filter off and refill with preheated xylene. Vibrating happens with a 50 Hz vibrate mixer. By this the equilibrium (a diffusion proces) between unsolved polymer and the solution or solvent accelerates. In addition the temperature gradient in the vessel is minimized. The next fractionation temperature is reached in 20 °V/h. After that the whole sequence of vibrating, filtering off, filling and rinsing is repeated. During the filtering off of a fraction plus the rinsing step the xylene soluble fraction is slowly mixed in 1800 ml methanol under continuous stirring. The whole is stirred during one night. After precipitation of the polymer the whole is filtered over a 3 μm RC (regenerated Cellulose) filter. The polymer fraction is dried in a vacuum oven at 60 °C for 1 night and the mass was recorded.

2.3. Stress–strain measurements and data treatment

2.3.1. Sample preparation

The materials are pressed at 160 °C to a sheet with a thickness of about 300 μm.

The used procedure for pressing the materials is: 5 min heating up at 0 kN load, 3 min at 10 kN load, 3 min at 50 kN load and cooling down to room temperature at a load of 180 kN.

After pressing, the samples are annealed for 1 h at 120 °C and than slowly cooled down to room temperature by switching off the temperature chamber.

Finally the test specimens (ISO37 type 3) are punched from the pressed sheets.

2.3.2. The measurement

The measurement is in principle a standard tensile test. The test specimen is extended along its major axis at constant speed (10 mm/min) until the strain reaches 1200%. The maximum strain value is limited by the length of the temperature chamber. During the test the load sustained by

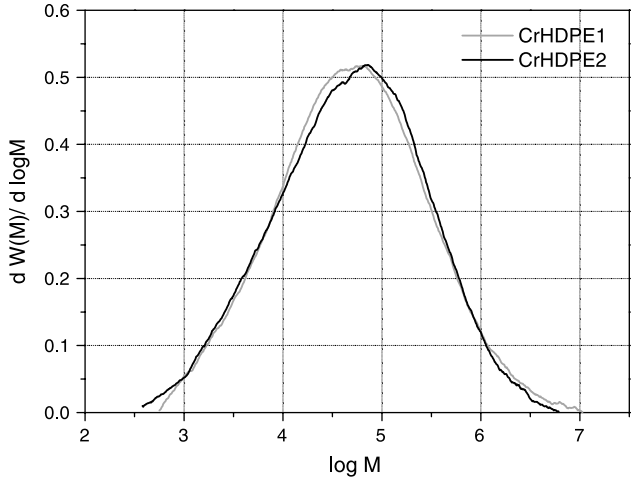

Fig. 1. Molar mass distribution of CrHDPE1 and CrHDPE2.

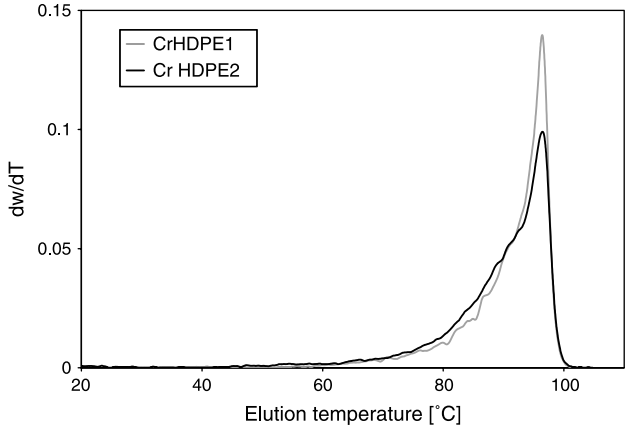

Fig. 2. TREF chromatographs of CrHDPE1 and Cr HDPE2.

the specimen and the elongation are measured. A 200N load cell is used for the load measurement. The elongation is determined with an optical extensometer. Therefore two reflecting and self-adhesive gauge marks are attached to the test specimens. The initial distance between these marks (gauge length) is determined after reaching the pre-load before each test.

Prior to testing the test specimen are kept for about 30 min in the temperature chamber at the envisaged test temperature so as to allow thermal equilibrium.

2.3.3. Data treatment

Lambda (true strain) is calculated on the basis of the gauge length:

$$\lambda = \frac{\Delta L}{L_0} + 1$$

where λ is the true strain value expressed as a dimensionless ratio, L_0 is the initial distance between the gauge marks in millimetres and ΔL is the increase in the specimen length between the gauge marks in millimetres.

The true stress is calculated assuming conservation of sample volume between the gauge marks:

$$\sigma_t = \frac{F}{A\lambda}$$

where σ_t is the true stress in MPa, F is the measured force in Newtons, A is the initial cross-sectional area of the specimen in square millimetres and λ is the true strain value expressed as a dimensionless ratio.

The strain hardening modulus $\langle G_p \rangle$ is calculated as the average difference quotient:

$$\langle G_p \rangle = \frac{1}{N} \sum_{i=1}^{N} \frac{\sigma_{i+1} - \sigma_i}{\lambda_{i+1} - \lambda_i}$$

The average runs over all N difference quotients between the start of the strain hardening part and below the maximum elongation of the stress–strain curve. The strain hardening part of the curve is considered to be the homogeneously deforming part well above the natural draw ratio, which is visually determined by observation of the neck propagation, and below the maximum draw ratio. The calculation of $\langle G_p \rangle$ for this study is performed typically between draw ratio's 9 and 12.

$\langle G_p \rangle$ is expressed in MPa.

2.4. ESCR measurement

A standard tensile ESCR test was performed at 75 °C applying constant stress of 3 MPa in a detergent solution (Rhodacal DS50) on a notched compression moulded sample. Sample dimensions are $63.5 \times 12.7 \times 1$ mm^3. A notch is punched in the middle of a sample, parallel with the short edges.

3. Results

3.1. Influence of comonomer incorporation in the samples possessing the same density and MFR but different ESCR (CrHDPE1 and CrHDPE2)

Samples CrHDPE 1 and CrHDPE2 are Phillips based HDPEs characterised by the same density, and MFR but significantly different ESCR. It is very well known that HDPE catalysed by Phillips catalyst is characterised by high inhomogeneity, as far as molar mass distributions as well as chemical composition distribution are concerned [23]. Before we proceed further with the differences in mechanical response of these samples molecular differences between the samples will be shortly discussed.

3.1.1. Molecular characterisation of CrHDPE1 and Cr HDPE2

As shown in Table 1 CrHDPE1 and CrHDPE 2 exhibit the same density and MFR. The molar mass distribution

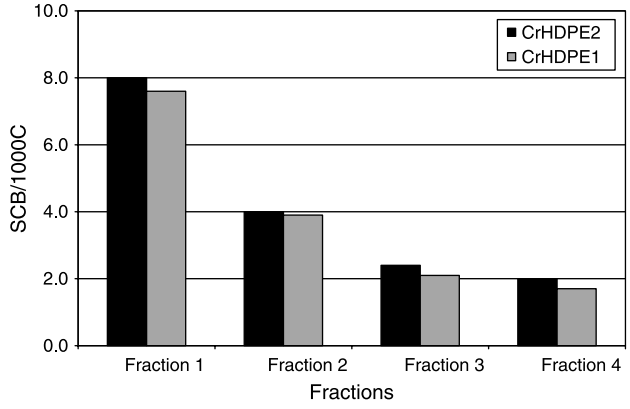

Fig. 3. The total amount of short chain branches (SCB/1000C atoms) per preparative TREF fraction determined by ^{1}H NMR.

(MMD) curves (Fig. 1) also show that the differences between the two samples are marginal.

Though the samples seem to be molecularly rather similar their mechanical performance (measured by ESCR) is significantly different. In order to understand the differences leading to different material performance the TREF fractionation, analytical and preparative, has been performed.

In Fig. 2 analytical TREF chromatograph, showing short chain branching distribution, of CrHDPE1 and Cr HDPE2 is displayed. The IR signal is reduced by the total surface area, which corrects possible inconsistencies related to the IR detector.

From this figure the differences between the two samples are obvious. The branched shoulder (60–94 °C) of CrHDPE2 is much more pronounced than for CrHDPE1. This result shows that despite the same density of the samples, CrHDPE2 possesses higher amount of short chain branched molecules. This is only possible if the comonomer incorporation in the higher molar mass portion of MMD is different for the two samples [23,39]. In order to get insight into possible variations in comonomer incorporation with respect to MMD preparative TREF fractions have been separated and SEC and ^{1}H NMR have been measured on these separate fractions.

The following four fractions have been separated based on the analytical TREF curve:

Fraction 1: 63–85 °C.
Fraction 2: 85–93.3 °C.
Fraction 3: 93.3–96.5 °C.
Fraction 4: 96.5–113 °C.

The amount of SCB measured for each separate fraction is given in Fig. 3.

It can be seen that the total amount of branches decreases from fraction 1 to fraction 3. No significant differences in

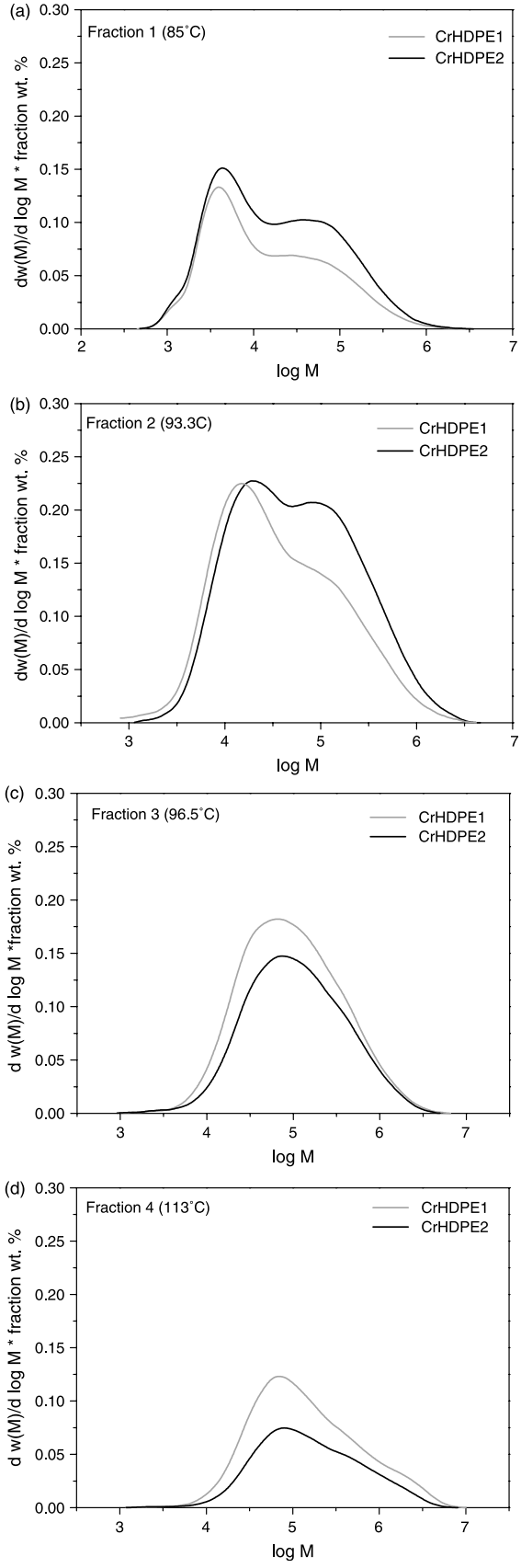

Fig. 4. Molar mass distribution curves normalised by the weight percentage of each separate fraction of Cr HDPE1 and Cr HDPE2. (a) Fractions 1 of Cr HDPE 1 and Cr HDPE2, (b) fractions 2 of Cr HDPE 1 and Cr HDPE2, (c) fractions 3 of Cr HDPE 1 and Cr HDPE2, (d) fractions 4 of Cr HDPE 1 and Cr HDPE2.

short chain branching could be seen between fraction 3 and fraction 4. According to Wilde [38] fractions above 95 °C should be rather linear, which in our case is not completely the case. This might be a consequence of certain blockiness in comonomer incorporation.

As indicated before, in order to trace molecular differences leading to different ESCR performance between CrHDPE1 and CrHDPE2, SEC of each separate fractions has been measured. In order to be able to compare comonomer incorporation of different samples the specific fractions are presented separately in Fig. 4(a)–(d). SEC curves in Fig. 4 are corrected for the fraction weight percentage in the respective sample.

SEC curves of fractions 1 and 2 (Fig. 4(a) and (b)) exhibit two SEC peaks, which has been observed before [39]. If one compares fractions 1 and 2 of the two respective samples (Cr HDPE1 and Cr HDPE2) it is obvious that the MMD of these fractions is much broader for CrHDPE2 than for CrHDPE1. This means that for CrHDPE2 the branched fractions are extended to a higher molar mass than in the case of CrHDPE1. Also the proportion of the branched fraction is higher in CrHDPE2 than in CrHDPE1. It has been shown previously that for a good ESCR performance the most ideal comonomer incorporation is in the high molar mass fraction, which favours the occurrence of intercrystalline effective tie molecules during crystallisation. However most of the supported catalyst (Ziegler-Natta or Phillips) incorporate comonomer units preferably into shorter chains leading to an inhomogeneous comonomer incorporation. This is the reason why for the high demanding applications like pipes, where ESCR values of >1000 h are required the bimodal grades are used, where incorporation of comonomer can be controlled by dosing comonomer preferentially in the second reactor, i.e. in the high molar mass portion of MMD [54,55]. Though lots of work has been done in studying molecular structure of Z-N catalysed systems, a very scarce amount of data can be found for Phillips catalyst systems. The results presented above show that in contrast to Ziegler Natta systems a substantial amount of branched molecules (SCB > 7SCB/1000C) are present in relatively high molar mass (up to 1×10^6 g/mol). Also the variations in

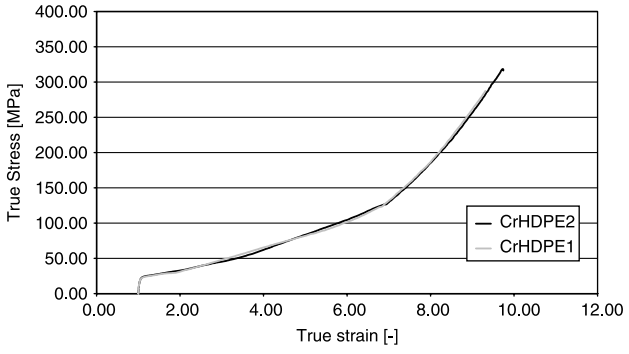

Fig. 5. Stress–strain curves expressed as true stress–true strain performed at room temperature at 10 mm/min.

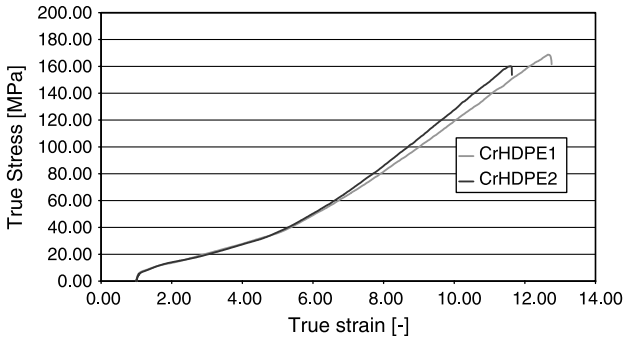

Fig. 6. Stress–strain curves expressed as true stress–true strain performed at 80 °C at 10 mm/min.

the amount of the branched fractions as well as subtle differences in their molar mass distribution can lead to significantly different material performance. Such subtle differences in comonomer incorporation in longer chains obviously lead to differences in ESCR without changing the overall density.

Fig. 4(c) and (d) shows SEC curves of the more linear fractions (fraction 3 and 4). It can be seen that MMD of linear fractions in CrHDPE1 is broader, i.e. extended to higher values of molar mass. It is interesting to note that despite of the fact that CrHDPE1 has more pronounced long molar mass tail its ESCR performance is less than for CrHDPE2. These results show conclusively that ESCR is highly sensitive to the slightest differences in comonomer incorporation in the higher molar mass tail.

In that sense Phillips based HDPEs are rather unique due to their heterogeneity in molar mass distribution as well as chemical composition distribution leading to significant differences in material performance [23,39,40].

3.1.2. Tensile response of CrHDPE1 and CrHDPE2

Stress–strain curves of samples CrHDPE1 and CrHDPE2, expressed in the form of true stress–true strain curves (TS–TS), obtained at the strain rates of 10 mm/min are given in Fig. 5.

The stress–strain response of CrHDPE1 and CrHDPE2 at standard tensile test conditions i.e. a traverse displacement of 10 mm/min at room temperature do not differ significantly. Under these conditions no significant variations in tensile response are expected considering the basic molecular similarities of the two materials (Table 1).

When the stress–strain curves of the same two materials are measured at 80 °C, which is a temperature at which most of the standard ESCR tests are performed, and at a constant test speed of 10 mm/min an obvious difference between two curves becomes noticeable as shown in Fig. 6.

At low draw ratios (up to their yield point) the curves are the same, which is expected considering the fact that the overall crystallinity (density) of the two specimens is identical [41]. The draw ratio region between the yield point and the draw ratio of about 5 features heterogeneous deformation (necking and neck propagation) and therefore

Table 2
ESCR data vs. $\langle G_p \rangle$ of the samples used in this study

Grades	ESCR (h)	SD	$\langle G_p \rangle$ (MPa)	SD
Cr HDPE1	58	6.3	18.8	0.4
Cr HDPE2	103	0.8	20.6	0.7
Cr HDPE3	10	0.8	13.1	0.2
Cr HDPE4	20	1.1	15.4	0.2
Cr HDPE5	50	2.1	19.0	0.2
Cr HDPE6	47	1.9	19.5	0.8
Cr HDPE7	112	12	26.0	1.1
Cr HDPE8	300	18	30.7	0.3
biHDPE1	1000	120	35.8	1.1
biHDPE2	>2000	n.d.	47.2	2.3

SD refers to standard deviation.

the true stress–true strain (TS–TS) treatment is not justified unless proper measures are taken to record the real local deformation as suggested by Haynes [42], Haward [43], G'Sell [44,45] Strobl et al. [46] and Ward et al. [47]. Because the scope of the present paper aims at using the strain hardening behaviour of the material as a measure of slow crack propagation, this heterogeneous part will not be considered in the further treatment. Once the upper and lower necks have propagated outside the optical markers the recorded strain is homogeneous and the TS–TS treatment is straightforward. At draw ratios above 5 an obvious difference between samples CrHDPE1 and CrHDPE2 can be observed for measurements performed at 80 °C. Sample CrHDPE2 features higher strain hardening than sample CrHDPE1. The same sample also exhibits a higher value of the notched ESCR test used for this purpose. Considering again the relationship between the creep rate of HDPE drawn to its natural draw ratio and notched ESCR [35] as well as the uniformity of strain–stress–strain rate surface [33,34] it is plausible to assume that the same parameters guiding the creep rate of HDPE drawn to the natural draw ratio also determine the strain hardening response of a material.

It is also remarkable to see that the tensile response of these two materials is sensitive enough to probe the subtle differences between the samples leading to different ESCR.

In order to associate the strain hardening response to ESCR a proper physical measure of strain hardening has been considered. Quantification of the strain hardening part of the curve based on rubberelastic network models has extensively been discussed in literature. As examples we mention the work of Haward [48,49] who uses Gaussian and 3-chain non-Gaussian rubber-elastic models, Brereton and Klein [50] who use Edwards Gaussian and non-Gaussian models. Other approaches involve phenomenological mechanical modelling such as Boyce's 8 chain model [51]. In order to assess the molecular differences in terms of fixed and slipping entanglement densities and entanglement slip parameters, which should then relate to the underlying molecular structure, the present set of stress–strain data were fitted with several of these models. It was however found that a Gaussian description remains valid well above draw ratios of 6, from which it can be concluded that the observed strain hardening does not follow the physics of a network system and hence these models cannot be used.

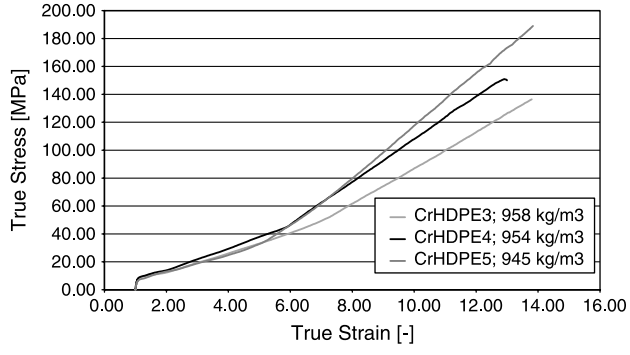

Fig. 7. Stress–strain curves of CrHDPE3, CrHDPE4 and CrHDPE5, expressed as a true stress–true strain, performed at 80 °C at 10 mm/min.

Since it is not the scope of this work to physically explain the strain hardening behaviour but merely to relate it to the ESCR score of a material we will limit ourselves to record a simple stable mathematical measure for the observed strain hardening, i.e. the average slope, which will be referred to as $\langle G_p \rangle$. The determination of $\langle G_p \rangle$ is described in the Section 2. The results are given in Table 2. It is obvious that the slope of strain hardening expressed as $\langle G_p \rangle$ is higher for the sample possessing higher ESCR.

3.2. Influence of comonomer content—the role of density

It has been shown in the previous section that the molecular details of comonomer incorporation are an important parameter determining ESCR performance of HDPE. In the previous section solely comonomer incorporation has been discussed in the samples possessing comparable total amount of short chain branches (SCB in Table 1). It is however, very well known that the total amount of short chain branching is also a parameter that ESCR is highly sensitive of. It is very well known that an increase in total amount of short chain branching leads to the lowering of density in final products [52]. This effect is associated with the fact that the short chain branches are largely excluded from a crystal leading to a disturbance of the regular chain folding [53]. Such disturbance leads not only to a decrease in crystallinity, but it also increases the number of tie molecules created upon crystallisation [20]. Therefore, slow crack propagation resistance is favoured by the lower [5,21,33,36] density (by increased total amount of short chain branches).

In Fig. 7 TS–TS curve of the materials possessing different density, i.e. different total amount of short chain branching (see Table 1 under SCB column), but comparable MFRs are displayed.

It can be observed from Fig. 7 that variations in short chain branching content (0.7–4.1 SCB/1000C) have a significant influence on the strain hardening modulus at

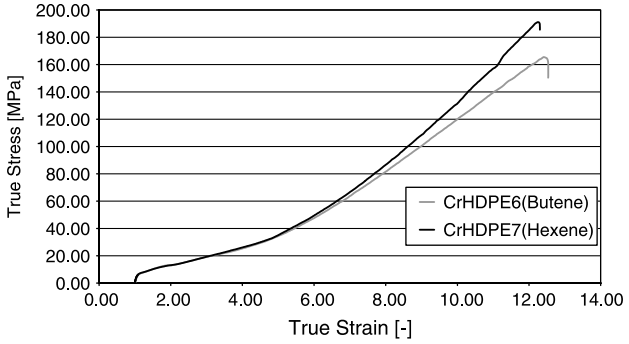

Fig. 8. Stress–strain curves of CrHDPE6 and CrHDPE7, expressed as a true stress–true strain, performed at 80 °C at 10 mm/min.

80 °C. The $\langle G_p \rangle$ values are given in Table 2. It can be seen from Table 1 that the ESCR values for these grades increase in the same sequence.

3.3. Influence of comonomer type (CrHDPE6 and CrHDPE7)

The size of a short chain branch plays also an important role in slow crack resistance of PE. The failure time of PE under the conditions of slow crack growth is shown to increase dramatically if the branch length is increased [22,40]. This is usually associated to the increased sliding resistance of the polymer chains through the crystal and/or entanglement in the amorphous region.

For the purpose of this study two samples possessing the same density and molecular characteristics have been synthesised with hexene and butene comonomer, respectively. The samples are identical as far as other material characteristics are concerned, as it can be seen in Table 1.

The TS–TS curves of CrHDPE6 and CrHDPE7 at 80 °C of these two samples are given in Fig. 8.

Also these two samples deviate significantly in the strain hardening region. CrHDPE7, synthesised with hexene as a co monomer strain hardens much steeper than the corresponding butene grade, inspite of the fact that ^{1}H NMR data show that hexene grades possesses somewhat lower amount of SCB/1000 (Table 1). As it can be seen in Table 1 CrHDPE7 possesses also much higher ESCR than the same sample prepared by butene as a comonomer. The calculated $\langle G_p \rangle$ values are given in Table 2.

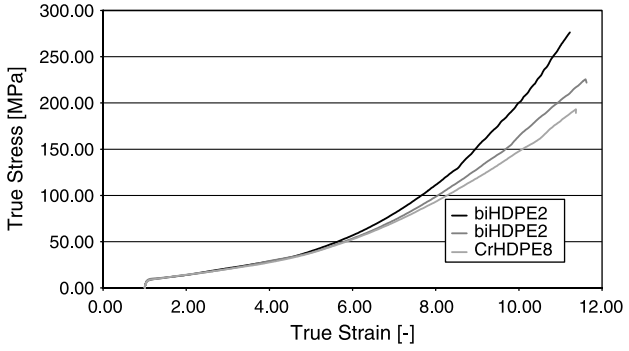

Fig. 9. Stress–strain curves of CrHDPE8, biHDPE1 and biHDPE2, expressed as a true stress–true strain, performed at 80 °C at 10 mm/min.

3.4. Pipe grades (CrHDPE8, biHDPE2, biHDPE3)

Another category of HDPEs where slow crack propagation is an important performance parameter are HDPE's used in pipe applications. Here slow crack propagation resistance is used in classification of HDPEs into different pipe classes like PE80 and PE100.

Long term crack resistance for classification of pipe grades of HDPEs is usually performed at elevated temperatures on pressurised pieces of pipes. Such tests last usually more than one year.

In order to assess information on slow crack propagation resistance of HDPE used in pipe applications the accelerated ESCR tests like FNCT test [24,31] are often used. However, the translation of these results to predicted lifetime of pipes is not always straightforward. Very often such tests for pipe grades are stopped after 1000 or 2000 h, which makes differentiation between grades extremely difficult.

For the purpose of this study three pipe grades have been selected, an unimodal Phillips based pipe material (CrHDPE8) and two bimodal grades, one belonging to PE80 (biHDPE1)and the other one to PE100 (biHDPE2) pipe grade category.

The stress–strain curves at 80 °C expressed as true stress–true strain curves are depicted in Fig. 9. The difference of the strain hardening part of the stress–strain curves is obvious. The unimodal Phillips based pipe grade (CrHDPE8) exhibits the lowest slope of the strain hardening part, corresponding the lowest value of $\langle G_p \rangle$. It should be noted that the selected unimodal grade possesses the lowest density and it is prepared by hexene as a comonomer. It has been shown in the previous sections that for the unimodal grades the both parameters favour higher ESCR performance. It is, however, very well known that bimodal processes used for synthesis of bimodal HDPE offer much more flexibility in tailoring material performance and therefore high demanding requirements needed for a grade to belong to PE100 class of pipe grades (withstanding stress of 10 MPa for 50 years at room temperature) can not be so far achieved by conventional unimodal processes [54,55]. From Fig. 9 it is obvious that both bimodal grades strain harden much more than the unimodal pipe grade. PE100 grade (biHDPE2) exhibits the highest slope of strain hardening, which is reflected in the ESCR value which can not be assessed by conventional ESCR measurements (ESCR > 2000 h).

4. Discussion

The results presented in the previous sections suggest that the average slope of strain hardening measured at 80 °C,

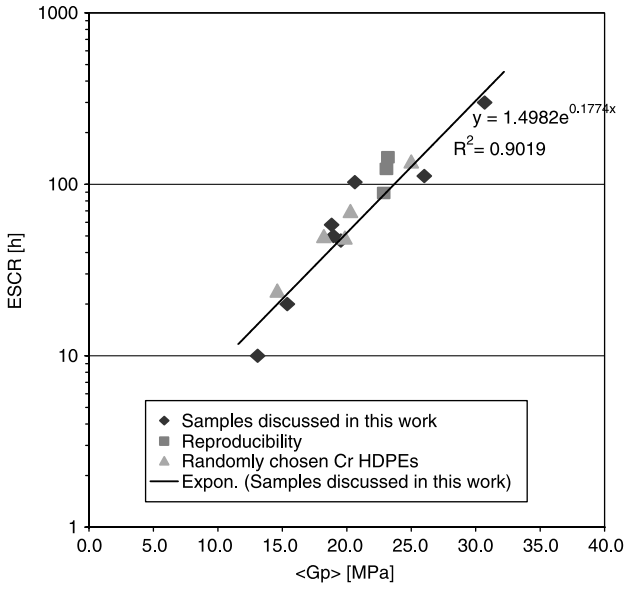

Fig. 10. Stress–strain curves of CrHDPE8, biHDPE1 and biHDPE2, expressed as a true stress–true strain, performed at 80 °C at 10 mm/min.

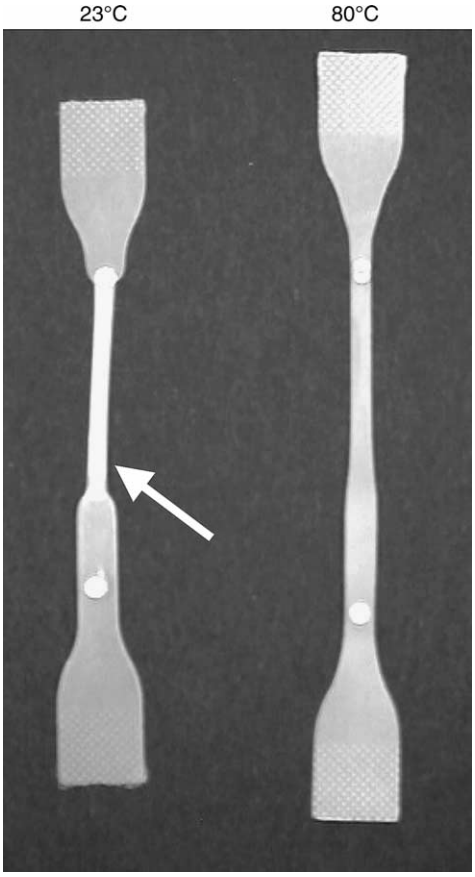

Fig. 11. A photograph of the propagated neck after the sample has been drawn to draw ratio of 3 at 23 °C and 80 °C. The arrow indicates typical necking at room temperature.

defined as $\langle G_p \rangle$, is sensitive to the same molecular differences that govern slow crack resistance in HDPE, measured by an accelerated ESCR test. In Table 2 the $\langle G_p \rangle$ values of all samples discussed in the previous sections are displayed. These data are plotted in Fig. 10 against ESCR values obtained by the accelerated ESCR test used in this study. Next to the data discussed in this paper also randomly selected Cr HDPE samples exhibiting a wider range of ESCR values are displayed in the same figure.

Fig. 10 nicely demonstrates that the accelerated ESCR data correlate amazingly well with $\langle G_p \rangle$ measured at 80 °C. Comparing these results with the results presented by Rose et al. [35,36], who showed very good agreement between ESCR data and the creep rate deceleration factor of polyethylene stretched to its natural drawn ratio, it is plausible to assume that the molecular and structural parameters governing creep of the drawn material are the same as those determining strain hardening at elevated temperature. The results of Rose et al. clearly show that the governing parameter in slow crack propagation of polyethylene is the creep rate of fibrils within a craze. Based on the concept of the unique strain–stress–strain rate surface introduced by O'Connel et al. [33] it is obvious that as the material increases in strain (and hence in true stress), the strain rate is decreasing and material is strain hardening. The material with strong strain hardening will reduce the strain rate and consequently the time to failure will be strongly increased. The data presented in this work provide experimental evidence for this concept by suggesting that slow crack propagation can be easily assessed by a simple parameter like the average strain hardening slope, as defined in this paper. The advantage of performing tensile tests at 80 °C is that the two processes responsible for the creep of oriented samples, like molecular disentanglement in the amorphous phase and sliding of the chains through the crystalline lamella [56], are emphasised. In this work it has been shown that the subtle differences in short chain branching in HDPE have a prominent influence on the amount of strain hardening at 80 °C and consequently their ESCR behaviour.

It should be noted that in some circumstances the same ranking of materials based on the slope of strain hardening could be observed at room temperature when measurements are performed at low traverse speeds like 0.2 mm/min. However, the results obtained at low traverse speeds are not always reliable. A possible explanation for this phenomenon might be the fact that stretching at elevated temperature lead to smoother necking as displayed in Fig. 11.

Besides the scientific relevance of the observed correlation presented in this work this approach offers a relatively easy way to predict the long-term service lifetime of HDPE products by a fast and well defined tensile experiment. The main advantage of this approach is its long-term reproducibility, which is rather questionable for the standard accelerated ESCR test using surfactants and notched samples. In Table 3 one single sample (CrHDPE9)

Table 3
ESCR and $\langle G_p \rangle$ data for CrHDPE9 measured at different times

Grades	ESCR (h)	SD	$\langle G_p \rangle$	SD	Date of measurement
Cr HDPE9	144	12	23.2	0.8	Nov-03
Cr HDPE9	89	7	22.9	0.4	Jan-04
Cr HDPE9	123	11	23.1	0.3	Mrt-04

is repeatedly tested following the conventional ESCR protocol and tensile test as described in this paper. These results are also displayed in Fig. 10 indicated as 'reproducibility' points. The difference in standard deviation of the results obtained by the accelerated ESCR as compared to the standard deviation in the tensile test results is convincingly clear.

It should also be mentioned that this new way of assessing ESCR data can be applied in any mechanical laboratory equipped with a tensile machine featuring a temperature chamber and an optical extensometer.

5. Conclusions

It has been shown in this paper that the average strain hardening slope $\langle G_p \rangle$ correlates with the data obtained by a classical accelerated ESCR test. The present results provide experimental evidence for the existence of the unique strain–stress–strain rate surface by offering a simple way to predict long term performance.

The experimental data performed on the critically selected samples show that the strain hardening at 80 °C is extremely sensitive to subtle molecular differences between different HDPE samples, notably extent and type of short chain branching and chemical composition distribution.

The reproducibility of the excellent correlation between ESCR and $\langle G_p \rangle$ suggests that the true stress–true strain response of a material is an intrinsic material property purely determined by its molecular structure parameters which are clearly the same parameters governing slow crack propagation in HDPE.

Moreover, this technique offers a relatively easy way of predicting long-term performance of ESCR without using surfactants and complicated sample preparation. Also measuring times are highly reduced (from few hundreds or thousands hours to only a few).

Acknowledgements

The authors would like to thank Prof I.M. Ward, IRC in Polymer Science and Technology at University of Leeds, for fruitful discussions related to this subject as well as his assistance in the preparation of this manuscript.

References

[1] Brown N, Bhatacharya SK. J Mater Sci 1985;20:4553–7.
[2] Lu X, Brown N. Polymer 1987;28(9):1505–11.
[3] Wang X, Brown N. Polymer 1988;29(3):463–6.
[4] Lu X, Wang X, Brown N. J Mater Sci 1988;23:643–8.
[5] Huang Y, Brown N. J Polym Sci, Part B: Polym Phys 1991;29:129–37.
[6] Boehm LL, Enderle HF, Fleissner M. Adv Mater 1992;4:231–8.
[7] Ward IM, Lu X, Huang Y, Brown N. Polymer 1991;32(12):2172–8.
[8] Lustiger A, Corneliusen RD. J Mater Sci 1987;22:2470–6.
[9] Lustiger A, Markham RL. Polymer 1983;24:1647–54.
[10] Kambour RP. Nature 1962;195(4848):1299–300.
[11] Argon AS, Salama MM. Philos Mag 1977;36:1217–34.
[12] Donald AM, Kramer EJ. Polymer 1982;23(3):457–60.
[13] Brown N, Lu X. Polymer 1995;36(3):543–8.
[14] Lu X, McGhie A, Brown N. J Polym Sci, Part B: Polym Phys 1992;30:1207–14.
[15] Brown N, Ward IM. J Mater Sci 1983;18:1405–20.
[16] Huang Y, Brown N. J Mater Sci 1988;23:3648–55.
[17] Egan BJ, Delatycki O. J Mater Sci 1995;30:3307–18.
[18] Egan BJ, Delatycki O. J Mater Sci 1995;30:3351–7.
[19] Lu X, Ishikawa N, Brown N. J Polym Sci, Part B: Polym Phys 1996;34:1809–13.
[20] Lustiger A, Ishikawa N. J Polym Sci, Part B: Polym Phys 1991;29:1047–55.
[21] Huang Y, Brown N. J Polym Sci, Part B: Polym Phys 1990;28:2007–21.
[22] Yeh JT, Chen CY, Hong HS. J Appl Polym Sci 1994;54:2171–86.
[23] Soares JBP, Abbot RF, Kim JD. J Polym Sci, Part B: Polym Phys 2000;38(10):1267–75.
[24] Fleissner M. Polym Eng Sci 1998;32:2172–81.
[25] Fleissner M. Polym Eng Sci 1998;38(2):330–40.
[26] Lagaron JM, Pastor JM, Kip BJ. Polymer 1999;40:1629–36.
[27] Boyd RH. Polymer 1985;26:1123–33.
[28] Chang P, Donovan A. Polym Eng Sci 1990;30(20):1431–41.
[29] Kramer EJ. Adv Polym Sci 1983;52/53:1–56.
[30] Bent strip test, ASTM standard D1693-70.
[31] Polyolefin pipes for the conveyance of fluids—determination of resistance to slow crack propagation—test method for slow rack growth on notched pipes, ISO 13479.
[32] Scholten GL, Pisters J, Venema B. Polym Testing 1989;8:385–405.
[33] O'Connell PA, Bonner MJ, Duckett RA, Ward IM. Polymer 1995;36:2355–62.
[34] O'Connell PA, Bonner MJ, Duckett RA, Ward IM. J Appl Polym Sci 2003;89:1663–70.
[35] Cawood MJ, Chanell AD, Capaccio G. Polym Commun 1993;32:423–5.
[36] Rose LJ, Channell CJ, Capaccio G. J Appl Polym Sci 1994;54:2119–24.
[38] Wild L. Adv Polym Sci 1990;98:1–47.
[39] Stephanne V, Daoust D, Debras G, Dupire M, Legras R, Michel J. J Appl Polym Sci 2001;82:916–28.
[40] Hubert L, David L, Seguela R, Vigier G, Degoulet C, Germain Y. Polymer 2001;42:8425–34.
[41] Brooks NW, Ghazali M, Duckett RA, Unwin AP, Ward IM. Polymer 1999;40(4):821–5.

[42] Haynes AR, Coates PD. J Mater Sci 1996;31:1843–55.
[43] Haward RN. Macromolecules 1993;26(22):5860–9.
[44] G'Sell C, Jonas JJ. J Mater Sci 1979;14:583–91.
[45] G'Sell C, Hiver JM, Dahoun A, Souahi A. J Mater Sci 1992;27: 5031–9.
[46] Hiss R, Hobeika S, Lynn C, Strobl G. Macromolecules 1999;32(13): 4390–403.
[47] Coates PD, Ward IM. J Mater Sci 1980;15:2897–914.
[48] Haward RN. Polymer 1999;40:5821–32.
[49] Haward RN. Macromolecules 1993;26:5860–9.
[50] Brereton MG, Klein PG. Polymer 1988;29:970–4.
[51] Arruda E, Boyce M. J Mech Phys Solids 1993;41(2):389–412.
[52] Balta-Calleja FJ, Hosemann R. J Polym Sci: Polym Phys 1980;18(5): 1159–65.
[53] Vanderhart DL, Perez E. Macromolecules 1986;19(17):1902–9.
[54] Böhm LL. Angew Chem Int 2003;42:5010–30.
[55] Scherrenberg R, Bilda D. Proceedings plastics pipes XII 2004.
[56] Ward IM. Adv Polym Sci 1985;70:1–70.